

2015-10-19

# Molecular and Ionic Clusters of Rubidium Fluoride: Theoretical Study of Structure and Vibrational Spectra

Abubakari, Ismail

Science Publishing Group

---

10.11648/j.ijctc.20150305.11

*Provided with love from The Nelson Mandela African Institution of Science and Technology*

See discussions, stats, and author profiles for this publication at: <https://www.researchgate.net/publication/283071970>

# Molecular and Ionic Clusters of Rubidium Fluoride: Theoretical Study of Structure and Vibrational Spectra

Article · October 2015

DOI: 10.11648/j.jjctc.20150305.11

CITATION

1

READS

109

3 authors:



Ismail Abubakari

Dodoma University

2 PUBLICATIONS 1 CITATION

[SEE PROFILE](#)



Tatiana Pogrebnaya

The Nelson Mandela African Institute of Science and Technology

50 PUBLICATIONS 99 CITATIONS

[SEE PROFILE](#)



Alexander Pogrebnoi

The Nelson Mandela African Institute of Science and Technology

62 PUBLICATIONS 285 CITATIONS

[SEE PROFILE](#)

Some of the authors of this publication are also working on these related projects:



We are working on dyes for solar cells application (theoretical computation) [View project](#)



Theoretical study of structure, vibration spectra and thermodynamic properties of cluster ions in vapors over alkali earth halides [View project](#)

# Molecular and Ionic Clusters of Rubidium Fluoride: Theoretical Study of Structure and Vibrational Spectra

Ismail Abubakari<sup>1, 2, \*</sup>, Tatiana Pogrebnaya<sup>1, 2</sup>, Alexander Pogrebnoi<sup>1, 2</sup>

<sup>1</sup>The Nelson Mandela African Institution of Science and Technology (NM – AIST), Arusha, Tanzania

<sup>2</sup>Dept. of Materials, Energy Science and Engineering, The NM - AIST, Arusha, Tanzania

## Email address:

ismailabubakari@yahoo.com (I. Abubakari), tatiana.pogrebnaya@nm-aist.ac.tz (T. Pogrebnaya), alexander.pogrebnoi@nm-aist.ac.tz (A. Pogrebnoi), pgamtp@mail.ru (A. Pogrebnoi)

## To cite this article:

Ismail Abubakari, Tatiana Pogrebnaya, Alexander Pogrebnoi. Molecular and Ionic Clusters of Rubidium Fluoride: Theoretical Study of Structure and Vibrational Spectra. *International Journal of Computational and Theoretical Chemistry*. Vol. 3, No. 5, 2015, pp. 34-44. doi: 10.11648/j.ijctc.20150305.11

**Abstract:** In this study, the geometrical structure and vibrational spectra of the trimer molecule  $\text{Rb}_3\text{F}_3$  and ionic clusters  $\text{Rb}_2\text{F}^+$ ,  $\text{RbF}_2^-$ ,  $\text{Rb}_3\text{F}_2^+$ , and  $\text{Rb}_2\text{F}_3^-$  were studied by density functional theory (DFT) with hybrid functional B3P86 and Møller–Plesset perturbation theory of second order (MP2). The effective core potential with Def2–TZVP (6s4p3d) basis set for rubidium atom and aug–cc–pVTZ (5s4p3d2f) basis set for fluorine atom were used. The triatomic ions have a linear equilibrium geometric structure of  $D_{\infty h}$  symmetry, whereas for pentaatomic ions  $\text{Rb}_3\text{F}_2^+$ ,  $\text{Rb}_2\text{F}_3^-$  and trimer molecule  $\text{Rb}_3\text{F}_3$  different isomers have been revealed. For the ions  $\text{Rb}_3\text{F}_2^+$ ,  $\text{Rb}_2\text{F}_3^-$  three isomers were confirmed to be equilibrium; the linear ( $D_{\infty h}$ ), the planar cyclic ( $C_{2v}$ ) and the bipyramidal ( $D_{3h}$ ) while for trimer  $\text{Rb}_3\text{F}_3$ , two isomers were found; the hexagonal ( $D_{3h}$ ) and the “butterfly-shaped” ( $C_{2v}$ ) configuration.

**Keywords:** Geometrical Structure, Vibrational Spectra, Ionic Clusters, Hybrid Functional, Density Functional Theory, Møller–Plesset Perturbation Theory, Effective Core Potential, Isomers, Basis Set

## 1. Introduction

Rubidium halides  $\text{RbX}$  (X is a halogen) may form molecular and ionic clusters in saturated vapours. These species are characterized by different geometric structures, vibrational spectra, and thermodynamic properties depending on the number of atoms comprising the species [1]. Other properties of clusters like electronic, optical, magnetic, and structural are strongly depend on their size and composition [2, 3] thus the possibility that materials with desired properties can be made is accustomed by changing the magnitude and structure of the cluster aggregates [4]. Extensive studies of the properties of alkali halide cluster ions had been done previously using different methods [5–15]. High temperature mass spectrometry is well known as a successful method for investigation of ionic clusters in gaseous phase [16–22]. Some ions  $\text{M}_2\text{X}^+$ ,  $\text{MX}_2^-$ ,  $\text{M}_3\text{X}_2^+$  and  $\text{M}_2\text{X}_3^-$  were already recorded in vapours over alkali metal halides [16, 17, 20, 22, 23]. The cluster ions and neutral molecules over rubidium halides have been detected and studied by mass spectrometric technique [20, 23, 24]. Theoretical quantum chemical methods have

been proved to be useful tools in attaining the characteristics of ions and molecules [1]. For the rubidium halides, quantum chemical methods have been used to study the structure and properties of some ionic clusters over rubidium iodide,  $\text{Rb}_2\text{I}^+$ ,  $\text{RbI}_2^-$ ,  $\text{Rb}_3\text{I}_2^+$  and  $\text{Rb}_2\text{I}_3^-$  [15] and rubidium chloride,  $\text{Rb}_2\text{Cl}^+$ ,  $\text{RbCl}_2^-$ ,  $\text{Rb}_3\text{Cl}_2^+$ , and  $\text{Rb}_2\text{Cl}_3^-$  [25]. This study aims the theoretical investigation of neutral and ionic clusters of rubidium fluoride.

## 2. Methodology

The calculations were performed using the density functional theory (DFT) with hybrid functional the Becke–Perdew correlation B3P86 [26–29], and second order Møller–Plesset perturbation theory (MP2) implemented into PC GAMESS (General Atomic and Molecular Electronic Structure System) program [30] and Firefly version 8.1.0 [31]. The effective core potentials with Def2–TZVP (6s4p3d) basis set for Rb atom [32, 33] and aug–cc–pVTZ basis set

(5s4p3d2f) for F atom [32, 34] were used. The bases set were taken from the EMSL (The Environmental Molecular Sciences Laboratory, GAMESS US), Basis Set Exchange version 1.2.2 library [35, 36]. For visualisation of the geometrical structure, specification of parameters, and assignment of vibrational modes in infrared spectra the Chemcraft software [37] and MacMolPlt program [38] were applied.

The thermodynamic functions were calculated within the rigid rotator-harmonic oscillator approximation using the Openthermo software [39]. The values of energies  $\Delta_r E$  and enthalpies  $\Delta_r H^\circ(0)$  of the reactions were computed as follows:

$$\Delta_r E = \sum E_{i \text{ prod}} - \sum E_{i \text{ reactant}} \quad (1)$$

$$\Delta_r H^\circ(0) = \Delta_r E + \Delta_r \varepsilon \quad (2)$$

$$\Delta_r \varepsilon = 1/2hc(\sum \omega_{i \text{ prod}} - \sum \omega_{i \text{ reactant}}) \quad (3)$$

where  $\sum E_{i \text{ prod}}$ ,  $\sum E_{i \text{ reactant}}$  are the sums of the total energies of the products and reactants respectively,  $\Delta_r \varepsilon$  is the zero point vibration energy correction,  $\sum \omega_{i \text{ prod}}$  and  $\sum \omega_{i \text{ reactant}}$  are the sums of the vibration frequencies of the products and reactants respectively.

### 3. Results and Discussion

#### 3.1. Diatomic RbF and Dimer Rb<sub>2</sub>F<sub>2</sub> Molecules

To come up with the more appropriate methods to be used for calculations, three different DFT hybrid functionals, B3LYP5, B3P86 and B3PW91 and Møller–Plesset perturbation theory (MP2) have been used in calculations of properties of the diatomic RbF and dimer Rb<sub>2</sub>F<sub>2</sub> molecules. Then the calculated properties have been compared with the experimental data to choose the best performing method to be used in complex ionic and molecular cluster of rubidium fluoride.

The calculated equilibrium geometrical parameters, normal vibrational frequencies, ionization energy and dipole moments of the RbF molecule are shown in Table 1.

As is seen in Table 1, the internuclear distance ( $R_e$ ) of the diatomic molecule RbF computed using all methods are highly overrated, longer than the reference data by  $\sim 0.08$ – $0.09$  Å; the values of frequency ( $\omega_e$ ) are underrated by  $14$ – $27$  cm<sup>-1</sup> ( $\sim 5$ – $7\%$ ) if compared with the experimental data; the values of the dipole moment ( $\mu_e$ ) are overrated by  $\sim 0.6$ – $1.5$  D.

The values of the ionization energies, adiabatic  $IE_{ad}$  and vertical  $IE_{vert}$ , were obtained as the energy difference of the RbF<sup>+</sup> ion and neutral molecule; for the adiabatic  $IE_{ad}$  internuclear separation  $R_e(\text{Rb-F})$  was optimized both for neutral and ionic species, while the vertical  $IE_{vert}$  was calculated using the optimized value of  $R_e(\text{Rb-F})$  in neutral molecule only and accepted the same for the ion.

Table 1. Properties of the RbF molecule.

Property	B3LYP5	B3P86	B3PW91	MP2	Ref. data
$R_e(\text{Rb-F})$	2.364	2.347	2.352	2.356	2.2703 [40]
$-E$	123.97635	124.03424	124.02145	123.31829	
$\omega_e(\Sigma_u^+)$	349	357	353	362	376 [41, 42]
$\mu_e$	9.2	9.1	9.1	9.5	8.5131 [43]
$IE_{vert}$	9.44	9.59	9.45	9.66	
$IE_{ad}$	8.96	9.08	8.92		

Notes: Here and hereafter,  $R_e$  is the equilibrium internuclear distance (Å),  $E$  is the total electron energy (au),  $\omega_e$  is the fundamental frequency (cm<sup>-1</sup>),  $\mu_e$  is the dipole moment (D),  $IE_{vert}$  and  $IE_{ad}$  are the ionization energies, vertical and adiabatic, respectively (eV).

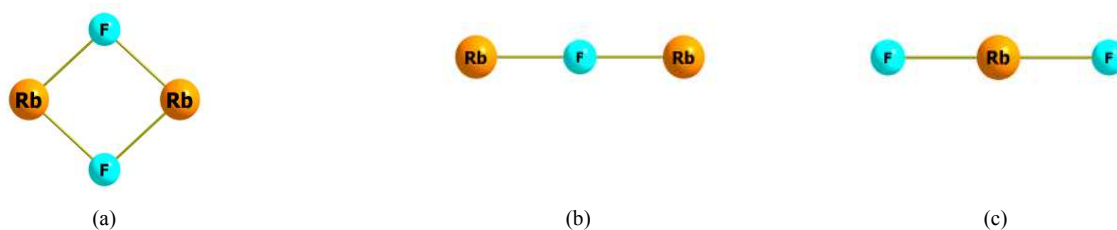


Figure 1. Equilibrium geometric structures: (a) Rb<sub>2</sub>F<sub>2</sub>; (b) Rb<sub>2</sub>F<sup>+</sup>; (c) RbF<sub>2</sub><sup>-</sup>.

The  $IE_{ad}$  by MP2 method was not found in this study because the optimization procedure by MP2 was not implemented for the species with multiplicity more than 1 in the software [30, 31]. The reference data on the  $IE$  of RbF to the best of our knowledge are not available. The theoretical values on  $IE_{vert}$  as well as  $IE_{ad}$  found by all four methods are in a good agreement with each other, respectively,  $IE_{vert}$  being by  $\sim 0.5$  eV higher than  $IE_{ad}$ .

For the dimeric molecule Rb<sub>2</sub>F<sub>2</sub> the structure was confirmed

to be planar of  $D_{2h}$  symmetry (Fig. 1a); the results are tabulated in Table 2. The geometrical parameters and vibrational frequencies calculated by different methods are in accordance with each other and literature data [44, 45] as well.

The IR spectrum of Rb<sub>2</sub>F<sub>2</sub> calculated by the MP2 method is shown in Fig. 2. Three peaks observed are assigned to asymmetrical stretching Rb–F modes at  $248$  cm<sup>-1</sup> and  $289$  cm<sup>-1</sup>, and bending out of plane vibration at  $91$  cm<sup>-1</sup>. Among these three IR active modes, two have highest intensity and

correspond to those which had been measured experimentally in IR spectrum in Ar matrix [45].

The dissociation reaction  $\text{Rb}_2\text{F}_2 \rightarrow 2\text{RbF}$  was considered and energy and enthalpy of the reaction was calculated using Eqs. (1)–(3). The values of  $\Delta_r H^\circ(0)$  found are in fair agreement with the reference data obtained from IVTANTHERMO database [46], the best result by the MP2 being overrated by  $2 \text{ kJ}\cdot\text{mol}^{-1}$ .

In conclusion of this section we can state that the data obtained by MP2 and DFT/B3P86 for the diatomic RbF and dimer  $\text{Rb}_2\text{F}_2$  molecules, agree better with the available reference experimental data as compared with other DFT hybrid functionals considered. Therefore DFT/B3P86 and MP2 methods were chosen for further computations of other ionic and molecular clusters.

**Table 2.** Properties of the dimer  $\text{Rb}_2\text{F}_2$  molecule of  $D_{2h}$  symmetry.

Property	B3LYP5	B3P86	B3PW91	MP2	Ref. data
$R_e(\text{Rb-F})$	2.553	2.534	2.542	2.527	2.527 [44] <sup>a</sup>
$\alpha_e(\text{F-Rb-F})$	83.7	83.7	83.9	83.0	82.2 [44] <sup>a</sup>
$-E$	248.02449	248.14023	248.11280	247.47912	
$\Delta_r E$	188.5	188.4	183.5	192.8	
$\Delta_r H^\circ(0)$	185.1	185.6	180.8	189.7	187.6 [46]
$\omega_1(A_g)$	250	255	250	265	
$\omega_2(A_g)$	101	101	101	107	
$\omega_3(B_{1g})$	221	227	221	245	
$\omega_4(B_{1u})$	86	87	86	91	
$\omega_5(B_{2u})$	232	238	233	248	230 [45]
$\omega_6(B_{3u})$	268	275	269	289	266 [45]

Notes: <sup>a</sup> The MP2 calculation. Here and hereafter,  $\alpha_e$  is the valence angle (deg).  $\Delta_r E$  and  $\Delta_r H^\circ(0)$  are the energy and enthalpy of the dissociation reaction ( $\text{kJ}\cdot\text{mol}^{-1}$ ). The reducible vibration representation reduces to  $\Gamma = 2A_g + B_{1g} + B_{1u} + B_{2u} + B_{3u}$ .

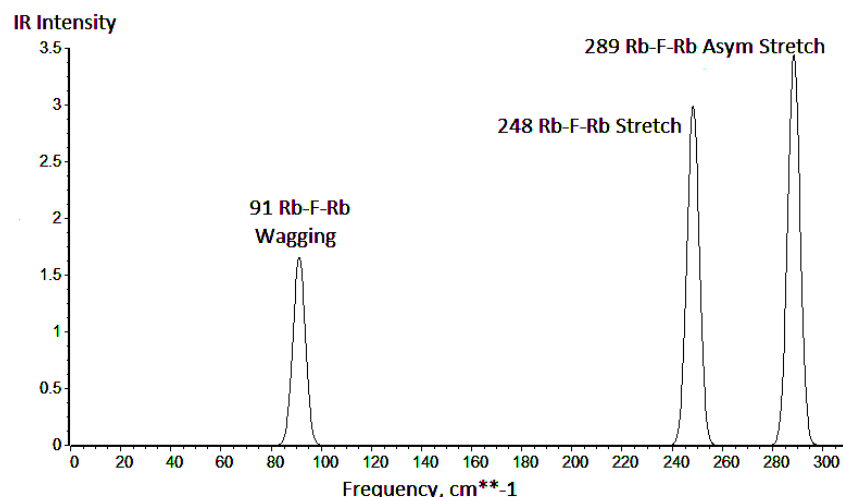


**Figure 2.** Theoretical IR spectrum of  $\text{Rb}_2\text{F}_2$  molecule ( $D_{2h}$ ); MP2 result.

**Table 3.** Properties of triatomic  $\text{Rb}_2\text{F}^+$  and  $\text{RbF}_2^-$  ions of linear symmetry  $D_{\infty h}$ .

Property	$\text{Rb}_2\text{F}^+$		$\text{RbF}_2^-$	
	B3P86	MP2	B3P86	MP2
$R_e(\text{Rb-F})$	2.481	2.479	2.540	2.534
$-E$	148.07834	147.50514	223.96693	223.54366
$\omega_1(\Sigma_g^+)$	126	128	244	253
$\omega_2(\Sigma_u^+)$	368	379	257	275
$\omega_3(\Pi_u)$	78	80	35	43
$I_2$	3.10	3.05	3.59	3.62
$I_3$	1.85	1.90	3.62	3.70

Note: Here and hereafter,  $I_i$  are the infrared intensities ( $\text{D}^2\cdot\text{amu}^{-1}\cdot\text{\AA}^{-2}$ ). The reducible vibration representation reduces to  $\Gamma = \Sigma_g^+ + \Sigma_u^+ + \Pi_u$

### 3.2. Triatomic $\text{Rb}_2\text{F}^+$ and $\text{RbF}_2^-$ Ions

Two structures were considered, linear of  $D_{\infty h}$  symmetry and

V-shaped of  $C_{2v}$  symmetry; the latter converged to linear during optimization and only linear structure was proved to be equilibrium (Figs. 1b, 1c). The calculated characteristics of the triatomic ions,  $\text{Rb}_2\text{F}^+$  and  $\text{RbF}_2^-$  are summarized in Table 3.

The values obtained by the two methods are generally in agreement with each other. By comparing positive and negative triatomic ions, the internuclear distance in negative ion  $\text{RbF}_2^-$  is longer by approximately  $0.06 \text{ \AA}$  due to an extra negative charge; in accordance to this the asymmetrical valence vibrational frequency  $\omega_2$  is higher for positive ion than for negative. The deformational frequency  $\omega_3$  of the negative ion is almost twice less compared the positive ion, that indicates the floppy deformational potential of the  $\text{RbF}_2^-$  ion. When compared with the similar ions for CsF [14], it may be noted the linear structure for  $\text{Cs}_2\text{F}^+$  alike  $\text{Rb}_2\text{F}^+$  and floppy

V-shaped structure of  $\text{CsF}_2^-$  with the angle of about  $150^\circ$ . In the spectra of these ions for CsF a correspondence between frequencies of the positive and negative triatomic ions is similar to that of the ions for RbF.

### 3.3. Pentaatomic $\text{Rb}_3\text{F}_2^+$ and $\text{Rb}_2\text{F}_3^-$ Ions

A number of possible geometrical configurations were

**Table 4.** Properties of pentaatomic  $\text{Rb}_3\text{F}_2^+$  and  $\text{Rb}_2\text{F}_3^-$  ions of linear symmetry  $D_{\infty h}$ .

Property	$\text{Rb}_3\text{F}_2^+$		Property	$\text{Rb}_2\text{F}_3^-$	
	B3P86	MP2		B3P86	MP2
$R_{e1}(\text{Rb}_2\text{-F}_3)$	2.442	2.443	$R_{e1}(\text{Rb}_1\text{-F}_4)$	2.492	2.492
$R_{e2}(\text{Rb}_1\text{-F}_3)$	2.587	2.571	$R_{e2}(\text{Rb}_1\text{-F}_3)$	2.605	2.586
$-E$	272.16771	271.26450	$-E$	348.05476	347.30131
$\omega_1(\Sigma_g^+)$	80	84	$\omega_1(\Sigma_g^+)$	90	96
$\omega_2(\Sigma_g^+)$	362	374	$\omega_2(\Sigma_g^+)$	284	292
$\omega_3(\Sigma_u^+)$	139	147	$\omega_3(\Sigma_u^+)$	278	285
$\omega_4(\Sigma_u^+)$	350	367	$\omega_4(\Sigma_u^+)$	297	321
$\omega_5(\Pi_g)$	62	64	$\omega_5(\Pi_g)$	21	27
$\omega_6(\Pi_u)$	(2)	3	$\omega_6(\Pi_u)$	17	19
$\omega_7(\Pi_u)$	71	77	$\omega_7(\Pi_u)$	52	61
$I_3$	0.03	0.00	$I_3$	4.22	3.32
$I_4$	6.21	6.11	$I_4$	2.42	3.31
$I_6$	(0.02)	0.05	$I_6$	1.54	1.63
$I_7$	3.58	3.63	$I_7$	3.95	3.98

Note: The reducible vibration representation for both positive and negative ions reduces to  $\Gamma = 2\Sigma_g^+ + 2\Sigma_u^+ + \Pi_g + 2\Pi_u$

The linear isomer is specified with two non-equivalent internuclear distances, terminal  $R_{e1}$  and bridged  $R_{e2}$ . For both positive and negative ions, the terminal distance is shorter than bridged one by  $\sim 0.10\text{--}0.15$  Å. The linear structure was proved to be equilibrium by the absence of imaginary frequencies for negative ion and for positive according to MP2 calculations. At the same time in the DFT calculation of linear  $\text{Rb}_3\text{F}_2^+$  ion, the value of  $\omega_6$  was imaginary. Nevertheless during the optimization procedure the bent structure of  $\text{Rb}_3\text{F}_2^+$  converged into slightly nonlinear without energy gain compared to linear, hence the linear configuration was accepted for this ion with the estimated value of  $\omega_6 \approx 2$   $\text{cm}^{-1}$ .

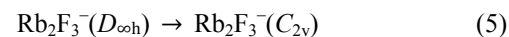
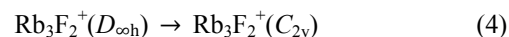
The existence of very low frequencies in the vibrational spectra of the linear pentaatomic isomers implies the floppy nonrigid structure of these species with shallow bending potential. For such species the entropy is assumed to be rather high and, based on the thermodynamic approach, the linear isomers are expected to prevail in saturated vapour compared to others. The IR spectra of the  $\text{Rb}_3\text{F}_2^+$  and  $\text{Rb}_2\text{F}_3^-$  ions ( $D_{\infty h}$ ) are shown in Fig. 4. For both ions four modes are active in IR spectra, and for the negative ion all of them are observed. For positive ion only two peaks at  $\omega_4 = 367$   $\text{cm}^{-1}$  and  $\omega_7 = 77$   $\text{cm}^{-1}$  are seen, while remaining two modes  $\omega_3$  and  $\omega_6$  are not displayed due to very low intensities.

The properties for planar cyclic structure are given in Table 5. There are three non-equivalent internuclear distance  $R_{e1}$ ,  $R_{e2}$  and  $R_{e3}$  and two valence angles  $\alpha_c$  and  $\beta_c$  (Figs. 3c, 3d) to specify the geometric configuration. The equilibrium internuclear distances of the negative ion are slightly greater than those of positive ion. Regarding the vibrational spectra of

considered for the pentaatomic ions  $\text{Rb}_3\text{F}_2^+$  and  $\text{Rb}_2\text{F}_3^-$ , linear of  $D_{\infty h}$  symmetry, V-shaped of  $C_{2v}$  symmetry, planar cyclic of  $C_{2v}$  symmetry, and bipyramidal of  $D_{3h}$  symmetry. Among them three structures were confirmed to be equilibrium, linear ( $D_{\infty h}$ ), planar cyclic ( $C_{2v}$ ), and bipyramidal ( $D_{3h}$ ), they are shown in Fig. 3. The geometrical parameters and vibrational spectra are recorded in Tables 4–6.

$\text{Rb}_3\text{F}_2^+$  and  $\text{Rb}_2\text{F}_3^-$ , a similarity is seen among the respective frequencies and IR intensities as well.

Isomerization reactions from linear into cyclic configurations were considered:



The energy of each reaction is the relative energy  $\Delta E_{\text{iso}}$  of the cyclic isomer with respect to linear one. The values of  $\Delta E_{\text{iso}}$  (Table 5) obtained by DFT and MP2 methods are slightly different; the DFT overrates a bit the energy of the cyclic isomer compared to MP2 method. Relying on the latter results, the energy of the cyclic isomer, is higher by  $5.0$   $\text{kJ}\cdot\text{mol}^{-1}$  for the  $\text{Rb}_3\text{F}_2^+$  ion and lower by  $2.5$   $\text{kJ}\cdot\text{mol}^{-1}$  for  $\text{Rb}_2\text{F}_3^-$  compared to linear isomer. Hence the cyclic isomer of both ions is close by energy to the linear one.

All in all most of the properties of the cyclic isomers of positive and negative pentaatomic ions look alike.

Results for bipyramidal isomers are shown in Table 6. Only one equilibrium internuclear distance  $R_c(\text{Rb-F})$  and one valence angle are needed to specify the geometric configuration (Figs. 3e, 3f). The internuclear distances of positive and negative ion are almost the same within the same method of calculation. Valence angle at the vertex of the bipyramidal is obtuse for  $\text{Rb}_3\text{F}_2^+$  and acute for  $\text{Rb}_2\text{F}_3^-$ . This tells us that the positively charged bipyramidal ion is slightly flattened compared to negatively charged one.

For the bipyramidal structure, in the vibrational spectra the lowest frequencies are about  $70$   $\text{cm}^{-1}$  ( $\text{Rb}_3\text{F}_2^+$ ) and  $\sim 120$   $\text{cm}^{-1}$

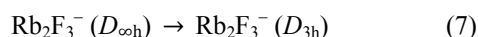
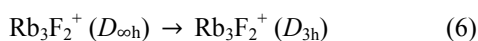
(Rb<sub>2</sub>F<sub>3</sub><sup>-</sup>). The absence of low frequencies in spectra and the bipyramidal shape itself indicate the rigidity and compactness of these isomers.

**Table 5.** Properties of pentaatomic Rb<sub>3</sub>F<sub>2</sub><sup>+</sup> and Rb<sub>2</sub>F<sub>3</sub><sup>-</sup> ions, planar cyclic isomers of C<sub>2v</sub> symmetry.

Property	Rb <sub>3</sub> F <sub>2</sub> <sup>+</sup>		Property	Rb <sub>2</sub> F <sub>3</sub> <sup>-</sup>	
	B3P86	MP2		B3P86	MP2
R <sub>e1</sub> (Rb <sub>2</sub> -F <sub>5</sub> )	2.467	2.464	R <sub>e1</sub> (Rb <sub>2</sub> -F <sub>4</sub> )	2.484	2.481
R <sub>e2</sub> (Rb <sub>2</sub> -F <sub>4</sub> )	2.787	2.748	R <sub>e2</sub> (Rb <sub>1</sub> -F <sub>4</sub> )	2.808	2.768
R <sub>e3</sub> (Rb <sub>1</sub> -F <sub>4</sub> )	2.503	2.505	R <sub>e3</sub> (Rb <sub>1</sub> -F <sub>3</sub> )	2.541	2.546
α <sub>c</sub> (Rb-F-Rb)	106.2	105.7	α <sub>c</sub> (F-Rb-F)	91.2	92.4
β <sub>c</sub> (F-Rb-F)	90.1	91.2	β <sub>c</sub> (Rb-F-Rb)	95.6	93.6
-E	272.16384	271.26261	-E	348.05431	347.30224
ΔE <sub>iso</sub>	10.2	5.0	ΔE <sub>iso</sub>	1.2	-2.5
ω <sub>1</sub> (A <sub>1</sub> )	295 (1.51)	308 (1.64)	ω <sub>1</sub> (A <sub>1</sub> )	271 (2.20)	280 (2.11)
ω <sub>2</sub> (A <sub>1</sub> )	73 (0.02)	77 (0.04)	ω <sub>2</sub> (A <sub>1</sub> )	78 (0.07)	82 (0.41)
ω <sub>3</sub> (A <sub>1</sub> )	91 (0.01)	99 (0.02)	ω <sub>3</sub> (A <sub>1</sub> )	79 (0.36)	82 (0.13)
ω <sub>4</sub> (A <sub>1</sub> )	263 (2.14)	271 (2.05)	ω <sub>4</sub> (A <sub>1</sub> )	249 (1.85)	258 (1.95)
ω <sub>5</sub> (B <sub>1</sub> )	105 (1.32)	110 (1.34)	ω <sub>5</sub> (B <sub>1</sub> )	123 (1.07)	145 (1.14)
ω <sub>6</sub> (B <sub>1</sub> )	39 (0.19)	38 (0.22)	ω <sub>6</sub> (B <sub>1</sub> )	25 (0.12)	26 (0.33)
ω <sub>7</sub> (B <sub>2</sub> )	311 (2.36)	322 (2.34)	ω <sub>7</sub> (B <sub>2</sub> )	291 (1.57)	299 (1.71)
ω <sub>8</sub> (B <sub>2</sub> )	134 (0.86)	156 (0.90)	ω <sub>8</sub> (B <sub>2</sub> )	158 (1.45)	175 (1.27)
ω <sub>9</sub> (B <sub>2</sub> )	40 (0.17)	42 (0.14)	ω <sub>9</sub> (B <sub>2</sub> )	53 (2.11)	52 (2.17)
μ <sub>c</sub>	5.4	5.9	μ <sub>c</sub>	4.8	5.4

Note: ΔE<sub>iso</sub> = E(C<sub>2v</sub>) - E(D<sub>∞h</sub>) is the relative energy of planar cyclic isomer regarding the linear one (kJ·mol<sup>-1</sup>). The values given in parentheses near the frequencies are infrared intensities (D<sup>2</sup>·amu<sup>-1</sup>·Å<sup>-2</sup>). The reducible vibration representation reduces into Γ = 4A<sub>1</sub> + 2B<sub>1</sub> + 3B<sub>2</sub>

For the isomerization reactions



the energies ΔE<sub>iso</sub> = E(D<sub>3h</sub>) - E(D<sub>∞h</sub>) are given in Table 6. The values of ΔE<sub>iso</sub> for positive and negative ions are negative, except Rb<sub>3</sub>F<sub>2</sub><sup>+</sup> by DFT. The negative values of ΔE<sub>iso</sub> indicate that the bipyramidal isomers are energetically more stable than linear isomers.

Thus three isomers for pentaatomic ions were revealed to exist. In order to come up with the conclusion of the most abundant isomer in saturated vapour, the relative concentrations were calculated using the following relation:

$$\Delta_r H^\circ(0) = -RT \ln(p_{\text{iso}}/p) + T \Delta_r \Phi^\circ(T) \quad (8)$$

where p<sub>iso</sub>/p is the ratio of the pressure of the cyclic or bipyramidal isomer to that of linear one, R is the gas constant, T is the absolute temperature, Δ<sub>r</sub>H<sup>°</sup>(0) and Δ<sub>r</sub>Φ<sup>°</sup>(T) are the enthalpy and change in the reduced Gibbs free energy of the isomerization reactions.

The reduced Gibbs free energy was found by the equation

$$\Phi^\circ(T) = -\frac{H^\circ(T) - H^\circ(0) - TS^\circ(T)}{T} \quad (9)$$

The thermodynamic functions, enthalpy increments H<sup>°</sup>(T) - H<sup>°</sup>(0), reduced Gibbs energies Φ<sup>°</sup> (J·mol<sup>-1</sup>·K<sup>-1</sup>), and entropies S<sup>°</sup>(T) were calculated for the temperature range 298–2000 K and gathered in Appendix. The required geometrical parameters and vibrational frequencies were used as obtained by MP2 method. The values of Δ<sub>r</sub>H<sup>°</sup>(0) for the isomerisation reactions (4)–(7) were found by Eqs. (1)–(3).

**Table 6.** Properties of pentaatomic Rb<sub>3</sub>F<sub>2</sub><sup>+</sup> and Rb<sub>2</sub>F<sub>3</sub><sup>-</sup> ions, bipyramidal isomers of D<sub>3h</sub> symmetry.

Property	Rb <sub>3</sub> F <sub>2</sub> <sup>+</sup>		Property	Rb <sub>2</sub> F <sub>3</sub> <sup>-</sup>	
	B3P86	MP2		B3P86	MP2
R <sub>e</sub> (Rb-F)	2.637	2.619	R <sub>e</sub> (Rb-F)	2.639	2.622
α <sub>c</sub> (Rb-F-Rb)	93.7	94.0	α <sub>c</sub> (F-Rb-F)	86.5	86.4
-E	272.16557	271.26800	-E	348.05871	347.31000
ΔE <sub>iso</sub>	5.6	-9.2	ΔE <sub>iso</sub>	-10.4	-22.8
ω <sub>1</sub> (A <sub>1</sub> )	264	273	ω <sub>1</sub> (A <sub>1</sub> )	242	252
ω <sub>2</sub> (A <sub>1</sub> )	114	121	ω <sub>2</sub> (A <sub>1</sub> )	125	126
ω <sub>3</sub> (A <sub>2</sub> )	207	216	ω <sub>3</sub> (A <sub>2</sub> )	210	221
ω <sub>4</sub> (E')	219	235	ω <sub>4</sub> (E')	216	229
ω <sub>5</sub> (E')	67	70	ω <sub>5</sub> (E')	117	119
ω <sub>6</sub> (E'')	157	176	ω <sub>6</sub> (E'')	142	158
I <sub>3</sub>	2.43	2.50	I <sub>3</sub>	3.50	3.62
I <sub>4</sub>	5.64	5.73	I <sub>4</sub>	5.57	5.65
I <sub>5</sub>	0.13	0.16	I <sub>5</sub>	1.64	1.71

Note: ΔE<sub>iso</sub> = E(D<sub>3h</sub>) - E(D<sub>∞h</sub>) is the relative energy of bipyramidal isomer regarding the linear one (kJ·mol<sup>-1</sup>). The reducible vibration representation reduces into Γ = 2A<sub>1</sub> + A<sub>2</sub> + 2E + E.

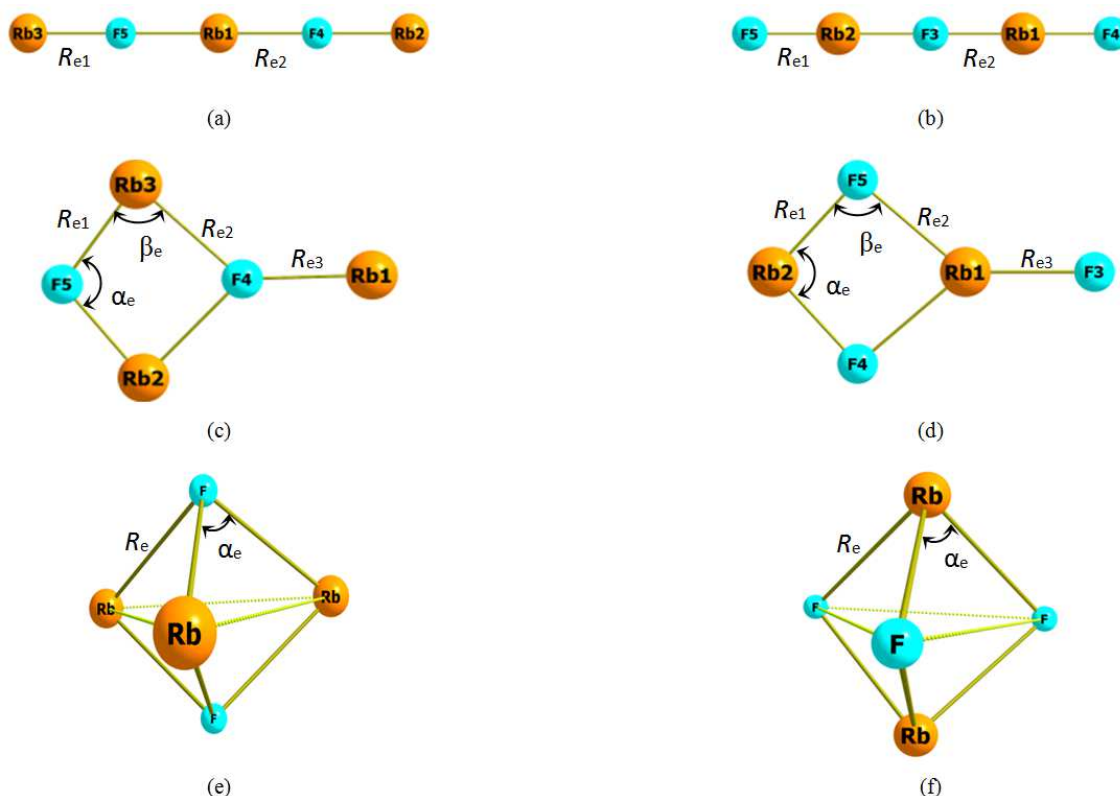


**Figure 3.** Geometrical structure of pentaatomic ions: (a) linear  $Rb_3F_2^+$ ; (b) linear  $Rb_2F_3^-$ ; (c) planar cyclic  $Rb_3F_2^+$ ; (d) planar cyclic  $Rb_2F_3^-$ ; (e) bipyramidal  $Rb_3F_2^+$ ; (f) bipyramidal  $Rb_2F_3^-$ .

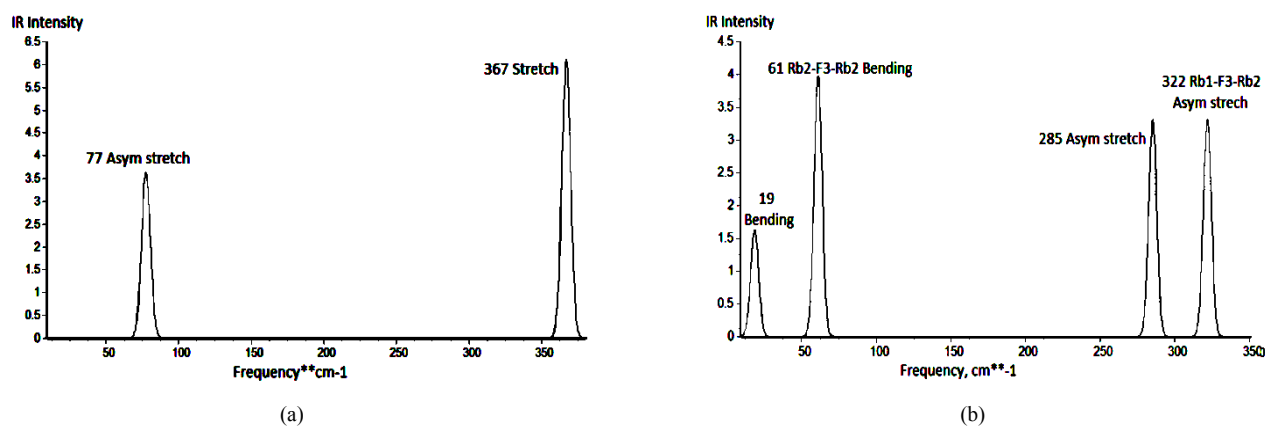


**Figure 4.** Theoretical IR spectra of pentaatomic ions ( $D_{\infty h}$ ) calculated by MP2 method: (a)  $Rb_3F_2^+$ ; (b)  $Rb_2F_3^-$ .

The values of  $p_{iso}/p$  were calculated for the temperature range between 700–1800 K; the plots for positive and negative ions are shown in Figs. 5a and 5b, respectively. As is seen the ratios  $p_{iso}/p$  are much less than 1 for all four cases. For the positive ion the amount of both cyclic and bipyramidal species is negligibly small and for the negative one it does not exceed 16% at 700 K and decreasing with temperature increase. Worth to note that the bipyramidal isomers are much less abundant in equilibrium vapour compared to linear despite they possess lower energy. It may be explained by prevailing of the competing entropy factor as it was predicted above. The existence of similar three isomeric forms was discussed previously regarding the pentaatomic ions over CsF

[14] and RbI [15] where the linear (or close to linear) isomers were proved to be predominant in equilibrium vapours. Therefore the entropy factor is significant to conclude which isomer is predominant in equilibrium vapour.

### 3.4. Trimer $Rb_3F_3$ Molecule

Three possible geometrical configurations were considered for trimer molecule,  $Rb_3F_3$ : linear of  $D_{\infty h}$  symmetry, hexagonal of  $D_{3h}$  symmetry and butterfly-shaped of  $C_{2v}$  symmetry. The linear structure appeared to be non-stable as imaginary frequencies were revealed. Two other configurations were confirmed to be equilibrium (Fig. 6). The obtained geometric parameters and vibrational frequencies for the hexagonal and



butterfly-shaped isomers are shown in Table 7. For the former, only one internuclear distance  $R_e(\text{Rb}-\text{F})$  and one valence angle are required to describe the structure while for the latter,

four internuclear distances and two valence angles are needed. The energy  $\Delta E_{\text{iso}}$  of the isomerization reaction

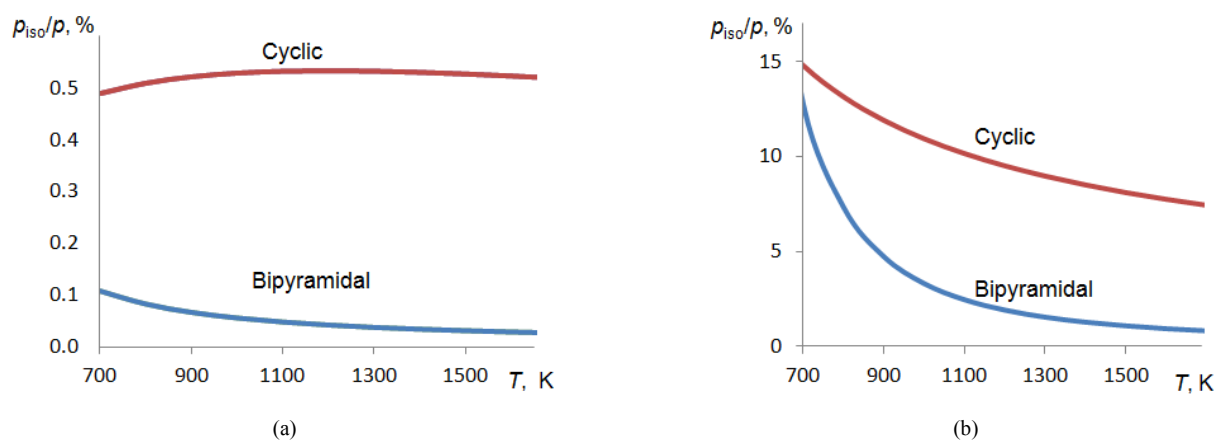
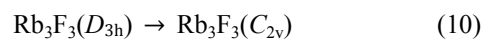


Figure 5. Temperature dependence of relative abundance of cyclic and bipyramidal isomers regarding linear: (a)  $\text{Rb}_3\text{F}_2^+$ ; (b)  $\text{Rb}_3\text{F}_3^-$ .

Table 7. Properties of trimer  $\text{Rb}_3\text{F}_3$  molecule, hexagonal ( $D_{3h}$ ) and butterfly-shaped ( $C_{2v}$ ).

Property	$\text{Rb}_3\text{F}_3 (D_{3h})$		Property	$\text{Rb}_3\text{F}_3 (C_{2v})$	
	B3P86	MP2		B3P86	MP2
$R_e(\text{Rb}-\text{F})$	2.536	2.529	$R_{e1}(\text{Rb}_1-\text{F}_4)$	2.484	2.479
			$R_{e2}(\text{Rb}_3-\text{F}_5)$	2.616	2.603
			$R_{e3}(\text{Rb}_2-\text{F}_6)$	2.576	2.566
			$R_{e4}(\text{Rb}_3-\text{F}_6)$	2.897	2.821
$\alpha_e(\text{Rb}-\text{F}-\text{Rb})$	128.3	129.1	$\alpha_e(\text{Rb}_2-\text{F}_5-\text{Rb}_3)$	99.7	99.5
$\beta_e(\text{F}-\text{Rb}-\text{F})$	111.7	110.9	$\beta_e(\text{F}_4-\text{Rb}_1-\text{F}_6)$	89.4	88.1
$-E$	372.23005	371.23920	$-E$	372.22917	371.24065
			$\Delta E_{\text{iso}}$	2.3	-3.8
$\omega_1(A_1')$	178	182	$\omega_1(A_1)$	286 (3.56)	295 (3.62)
$\omega_2(A_1')$	284	303	$\omega_2(A_1)$	118 (0.65)	140 (0.77)
$\omega_3(A_1')$	91	92	$\omega_3(A_1)$	111 (0.13)	117 (0.08)
$\omega_4(A_2'')$	82	84	$\omega_4(A_1)$	65 (0.09)	72 (0.04)
$\omega_5(E')$	313	328	$\omega_5(A_2)$	215	226
$\omega_6(E')$	187	193	$\omega_6(A_2)$	49	50
$\omega_7(E')$	40	38	$\omega_7(B_1)$	97 (2.00)	103 (2.02)
$\omega_8(E'')$	41	42	$\omega_8(B_1)$	15 (0.21)	24 (0.22)
$I_4$	2.38	2.46	$\omega_9(B_2)$	312 (2.33)	329 (2.50)
$I_5$	6.71	6.84	$\omega_{10}(B_2)$	269 (0.42)	280 (0.17)
$I_6$	2.42	2.38	$\omega_{11}(B_2)$	220 (2.42)	237 (2.54)
$I_7$	0.64	0.70	$\omega_{12}(B_2)$	79 (0.21)	85 (0.22)
			$\mu_e$	7.9	8.4

Notes:  $\Delta E_{\text{iso}} = E(C_{2v}) - E(D_{3h})$  is the relative energy of the butterfly-shaped isomer regarding the hexagonal one ( $\text{kJ}\cdot\text{mol}^{-1}$ ). The reducible vibration representations for  $\text{Rb}_3\text{F}_3$  of  $D_{3h}$  and  $C_{2v}$  symmetry reduce as follows:  $\Gamma = 3A_1' + A_2'' + 3E' + E''$  and  $\Gamma = 4A_1 + 2A_2 + 2B_1 + 4B_2$ , respectively. For the  $C_{2v}$  butterfly-shaped isomer, the values given in parentheses near the frequencies are infrared intensities ( $\text{D}^2\text{amu}^{-1}\text{\AA}^{-2}$ ).



Figure 6. Geometrical structures of trimer  $\text{Rb}_3\text{F}_3$  molecule: (a) hexagonal of  $D_{3h}$  symmetry; (b) butterfly-shaped of  $C_{2v}$  symmetry.

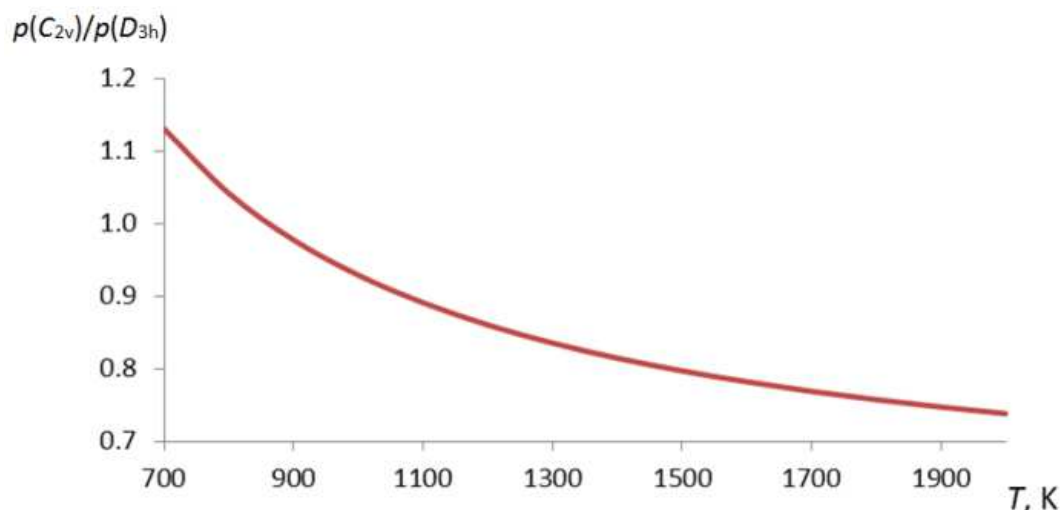


Figure 7. Temperature dependence of relative amount of the  $C_{2v}$  isomer regarding to  $D_{3h}$  isomer of trimer  $Rb_3F_3$  molecule.

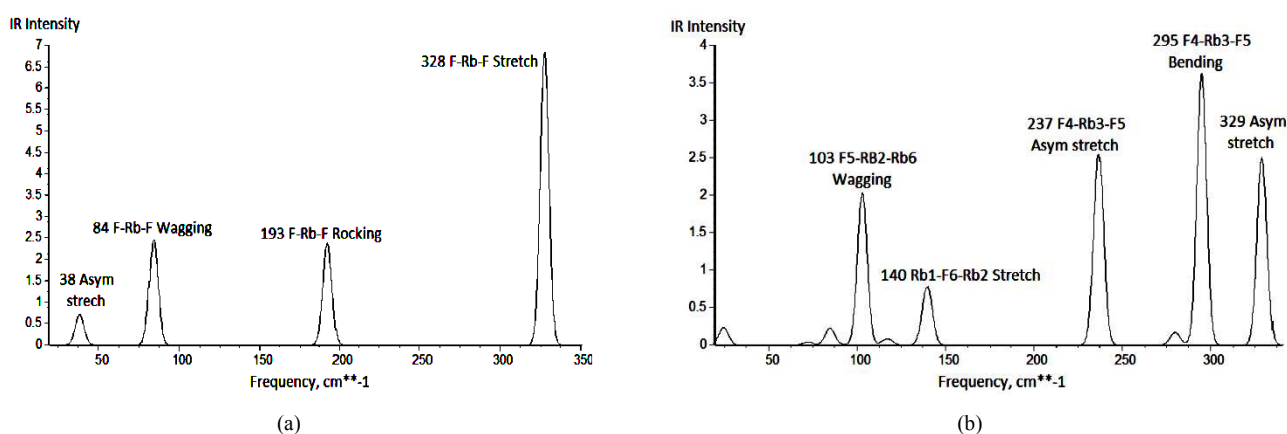


Figure 8. Theoretical IR spectra of the trimer  $Rb_3F_3$  molecule calculated by MP2 method: (a) hexagonal isomer ( $D_{3h}$ ); (b) butterfly-shaped isomer ( $C_{2v}$ ).

was determined. As compared to hexagonal, the butterfly-shaped configuration has a bit higher energy, by 2.3  $\text{kJ}\cdot\text{mol}^{-1}$ , according to DFT/B3P86 method, while it has a bit lower energy, by 3.8  $\text{kJ}\cdot\text{mol}^{-1}$ , according to MP2 method; that is these two isomers are close by energy to each other.

The relative concentrations of isomers have been determined similarly as it is described above in section 3.3. The ratio of  $p(C_{2v})/p(D_{3h})$  versus temperature is shown in Fig. 7. As is seen the ratio is close to one in a broad temperature range which means that two isomers compete with each other being in comparable amount. At low temperatures  $C_{2v}$  isomer show high abundance but its abundance decreases with temperature increase hence  $D_{3h}$  isomer seems to dominate at elevated temperatures. Worth to mention that similar isomeric structures were revealed for the  $Cs_3F_3$  molecule [14]: one hexagonal  $D_{3h}$  and the other of a “butterfly-shaped” ( $C_s$ ); the lower symmetry of the second of  $Cs_3F_3$  compared to  $Rb_3F_3$  apparently due to the bigger size and higher polarizability of the caesium atom.

The IR spectra of the trimer  $Rb_3F_3$  isomers are presented in Fig. 8. For the hexagonal isomer, only four modes are active in IR spectrum, and all of them are seen. In the spectrum of  $C_{2v}$  isomer all modes, except two,  $\omega_5$  and  $\omega_6$  of  $A_2$  symmetry, have

nonzero intensities but not all of them may be observed due to low intensities. For both isomers, the frequencies at  $\sim 200\text{ cm}^{-1}$  and above correspond to the stretching asymmetric vibrations Rb–F, the frequencies below  $100\text{ cm}^{-1}$  relate to bending vibration modes. The most intensive bands are assigned to the stretching Rb–F modes,  $328\text{ cm}^{-1}$  and  $295\text{ cm}^{-1}$  for the  $D_{3h}$  and  $C_{2v}$  isomers, respectively.

## 4. Conclusion

A number of molecular and ionic clusters, including the trimer  $Rb_3F_3$  molecule, triatomic  $Rb_2F^+$  and  $RbF_2^-$  and pentaatomic  $Rb_3F_2^+$  and  $Rb_2F_3^-$  ions, have been studied by DFT/B3P86 and MP2 methods. These methods were accepted for calculations of geometrical parameters and vibrational frequencies of the clusters because they provided a better agreement with the available reference data for diatomic RbF and dimer  $Rb_2F_2$  molecules. Alternative configurations have been considered for the molecular and ionic clusters. For the triatomic ions the linear structure ( $D_{\infty h}$ ) was confirmed to be equilibrium. The existence of isomers was proved for the pentaatomic ions and trimer molecule. The three isomers of comparable energy were revealed for  $Rb_3F_2^+$  and  $Rb_2F_3^-$  ions:

linear ( $D_{\infty h}$ ), planar cyclic ( $C_{2v}$ ), and bipyramidal ( $D_{3h}$ ), the linear one being the most abundant in the equilibrium vapour compared to others. Two isomeric forms of the trimer molecule  $Rb_3F_3$  were figured out: planar hexagonal ( $D_{3h}$ ) and butterfly-shaped ( $C_{2v}$ ); they were shown to have almost equal energy and comparable relative abundance in saturated vapour.

## Authors' Contributions

All authors participate well in all steps including computation, data analysis and manuscript preparation towards production of this work.

## Acknowledgment

The authors are thankful to the Tanzania Commission for Science and Technology (COSTECH) and The Nelson Mandela African Institution of Science and Technology (NM-AIST) for support and sponsorship of this work.

## Appendix

The thermodynamic functions of ionic and molecular clusters, triatomic ions  $Rb_2F^+$  and  $RbF_2^-$ , pentaatomic ions  $Rb_3F_2^+$  and  $Rb_2F_3^-$ , and trimer  $Rb_3F_3$  in gas phase are given in Tables A1–A6. The values of molar heat capacity  $c_p^\circ$ , entropy  $S^\circ$ , Gibbs reduced free energy  $\Phi^\circ$  are given in  $J\cdot mol^{-1}\cdot K^{-1}$ , and enthalpy increment  $H^\circ(T) - H^\circ(0)$  is in  $kJ\cdot mol^{-1}$ , absolute temperature  $T$  in K. The thermodynamic functions of the most abundant isomers only are given for the species existing in different isomeric forms.

Table A1. Thermodynamic functions of  $Rb_2F^+$  ( $D_{\infty h}$ ).

$T$	$c_p^\circ$	$S^\circ$	$H^\circ(T) - H^\circ(0)$	$\Phi^\circ$
298.15	59.92	304.811	15.398	253.167
700	61.86	356.979	40.013	299.818
800	61.98	365.248	46.205	307.492
900	62.06	372.553	52.407	314.323
1000	62.12	379.094	58.616	320.478
1100	62.15	385.017	64.829	326.081
1200	62.19	390.426	71.047	331.221
1300	62.20	395.405	77.267	335.969
1400	62.23	400.016	83.489	340.381
1500	62.25	404.310	89.713	344.501

Table A2. Thermodynamic functions of  $RbF_2^-$  ( $D_{\infty h}$ ).

$T$	$c_p^\circ$	$S^\circ$	$H^\circ(T) - H^\circ(0)$	$\Phi^\circ$
298.15	60.22	294.437	15.591	242.144
700	61.94	346.756	40.270	289.227
800	62.04	355.034	46.470	296.947
900	62.11	362.345	52.678	303.814
1000	62.16	368.891	58.891	310.000
1100	62.19	374.817	65.108	315.628
1200	62.22	380.230	71.329	320.790
1300	62.23	385.210	77.551	325.555
1400	62.25	389.823	83.776	329.983
1500	62.26	394.119	90.002	334.118

Table A3. Thermodynamic functions of  $Rb_3F_2^+$  ( $D_{\infty h}$ ).

$T$	$c_p^\circ$	$S^\circ$	$H^\circ(T) - H^\circ(0)$	$\Phi^\circ$
298.15	107.67	465.801	27.418	373.840
700	111.32	559.626	71.692	457.209
800	111.53	574.506	82.836	470.961
900	111.68	587.652	93.997	483.211
1000	111.79	599.425	105.171	494.254
1100	111.86	610.083	116.353	504.308
1200	-1492.90	619.819	127.543	513.533
1300	111.96	628.780	138.738	522.058
1400	112.01	637.079	149.937	529.981
1500	112.03	644.808	161.140	537.381

Table A4. Thermodynamic functions of  $Rb_3F_3^-$  ( $D_{\infty h}$ ).

$T$	$c_p^\circ$	$S^\circ$	$H^\circ(T) - H^\circ(0)$	$\Phi^\circ$
298.15	108.02	443.330	27.584	350.813
700	111.41	537.331	71.934	434.569
800	111.60	552.222	83.085	448.365
900	111.74	565.375	94.253	460.649
1000	111.84	577.154	105.432	471.722
1100	111.91	587.816	116.619	481.799
1200	111.96	597.556	127.813	491.045
1300	112.00	606.519	139.011	499.587
1400	112.03	614.821	150.213	507.526
1500	112.06	622.551	161.418	514.939

Table A5. Thermodynamic functions of  $Rb_3F_3$  ( $D_{3h}$ ).

$T$	$c_p^\circ$	$S^\circ$	$H^\circ(T) - H^\circ(0)$	$\Phi^\circ$
298.15	126.60	467.382	30.557	364.893
700	131.78	578.192	82.868	459.809
800	132.06	595.808	96.061	475.732
900	132.24	611.375	109.278	489.955
1000	132.42	625.319	122.513	502.806
1100	132.52	637.944	135.759	514.527
1200	132.59	649.478	149.015	525.299
1300	132.68	660.095	162.279	535.265
1400	132.74	669.928	175.547	544.537
1500	132.78	679.086	188.821	553.205

Table A6. Thermodynamic functions of  $Rb_3F_3$  ( $C_{2v}$ ).

$T$	$c_p^\circ$	$S^\circ$	$H^\circ(T) - H^\circ(0)$	$\Phi^\circ$
298.15	126.48	462.998	30.013	362.283
700	131.76	573.769	82.308	456.186
800	132.06	591.383	95.500	472.008
900	132.25	606.950	108.716	486.154
1000	132.40	620.893	121.950	498.943
1100	132.52	633.518	135.196	510.613
1200	132.60	645.051	148.452	521.341
1300	132.66	655.667	161.715	531.271
1400	132.72	665.500	174.983	540.512
1500	132.75	674.658	188.256	549.154

## References

- [1] Cramer, C. J. (2004), *Essentials of computational chemistry: theories and models*. John Wiley & Sons Ltd, 2<sup>nd</sup> Ed, USA.
- [2] Khanna, S. and Jena P., *Atomic clusters: Building blocks for a class of solids*. Phys. Rev. B. 1995. 51(19): p. 13705.
- [3] Khanna, S. and Jena P., *Assembling crystals from clusters*. Phys. Rev. Lett. 1993. 71(1): p. 208.

- [4] Rao, B., Khanna, S., & Jena, P., *Designing new materials using atomic clusters*. J. Cluster Sci. 1999. 10(4), 477-491.
- [5] Sarkas, H. W., Kidder, L. H., and Bowen, K. H., *Photoelectron spectroscopy of color centers in negatively charged cesium iodide nanocrystals*. J. Chem. Phys. 1995. 102(1): p. 57-66.
- [6] Alexandrova, A. N., Boldyrev, A. I., Fu, Y.-J., Yang, X., Wang, X.-B., & Wang, L.-S., *Structure of the  $Na_xCl_{x+1}$  ( $x=1-4$ ) clusters via ab initio genetic algorithm and photoelectron spectroscopy*. J. Chem. Phys. 2004. 121(12): p. 5709-5719.
- [7] Castleman, A. and Bowen K., *Clusters: Structure, energetics, and dynamics of intermediate states of matter*. J. Phys. Chem. 1996. 100(31): p. 12911-12944.
- [8] Castleman Jr, A., and Khanna, S., *Clusters, Superatoms, and Building Blocks of New Materials*. J. Phys. Chem. 2009. 113(7): p. 2664-2675.
- [9] Pogrebnoi, A. M., Pogrebnya, T. P., Kudin, L. S., & Tuyizere, S., *Structure and thermodynamic properties of positive and negative cluster ions in saturated vapour over barium dichloride*. Mol. Phys. 2013. 111(21): p. 3234-3245.
- [10] Hishamunda, J., Girabawe, C., Pogrebnya, T., & Pogrebnoi, A., *Theoretical study of properties of  $Cs_2Cl^+$ ,  $CsCl_2^-$ ,  $Cs_3Cl_2^+$ , and  $Cs_2Cl_3^-$  ions: Effect of Basis set and Computation Method*. Rwanda. Jornal. 2012. 25(1): p. 66-85.
- [11] Fernandez-Lima, F. A., Nascimento, M. A. C., and da Silveira, E. F., *Alkali halide clusters produced by fast ion impact. Nuclear Instruments and Methods in Physics Research Section B: Beam Interactions with Materials and Atoms*, 2012. 273: p. 102-104.
- [12] Huh, S., and Lee G., *Mass spectrometric study of negative, positive, and mixed KI cluster ions by using fast Xe atom bombardment*. J. Kor. Phys. Soc. 2001. 38(2): p. 107-110.
- [13] Aguado, A., *An ab initio study of the structures and relative stabilities of doubly charged  $[(NaCl)_m(Na)_2]^+$  cluster ions*. J. Phys. Chem. B, 2001. 105(14): p. 2761-2765.
- [14] Mwanga, S. F., Pogrebnya T. P., and Pogrebnoi, A. M., *Structure and properties of molecular and ionic clusters in vapour over caesium fluoride*. Mol. Phys. 2015. p.1-16.
- [15] Costa, R., Pogrebnya, T., and Pogrebnoi, A., *Structure and vibrational spectra of cluster ions over rubidium iodide by computational chemistry*. Pan African Conference on Computing and Telecommunications in Science (PACT). IEEE. 2014. PACTAT01114: pp. 52-55; doi: 10.1109/SCAT.2014.7055136.
- [16] Chupka, W. A., *Dissociation energies of some gaseous alkali halide complex ions and the hydrated ion  $K(H_2O)^+$* . J. Chem. Phys. 1959. 30(2): p. 458-465.
- [17] Kudin, L., Burdukovskaya, G., Krasnov, K., & Vorob'ev, O., *Mass spectrometric study of the ionic composition of saturated potassium chloride vapour. Enthalpies of formation of the  $K_2Cl^+$ ,  $K_3Cl_2^+$ ,  $KCl_2^-$ , and  $K_2Cl_3^-$  ions*. Russ. J. Phys. Chem. 1990. 64: p. 484-489.
- [18] Pogrebnoi, A., Kudin, L., Motalov, V., & Goryushkin, V., *Vapor species over cerium and samarium trichlorides, enthalpies of formation of  $(LnCl_3)_n$  molecules and  $Cl^-(LnCl_3)_n$  ions*. Rapid Communications in Mass Spectrometry, 2001. 15(18): p. 1662-1671.
- [19] Dunaev, A., Kudin, L., Butman, M. F., & Motalov, V., *Alkali Halide Work Function Determination by Knudsen Effusion Mass Spectrometry*. ECS Transactions, 2013. 46(1): p. 251-258.
- [20] Gusarov, A., *Equilibrium ionization in vapors of inorganic compounds and the thermodynamic properties of ions*. Chemical sciences doctoral dissertation, Moscow, 1986.
- [21] Sidorova, I., Gusarov, A., and Gorokhov, L., *Ion-molecule equilibria in the vapors over cesium iodide and sodium fluoride*. Intern. J. Mass Spec. Ion Phys. 1979. 31(4): p. 367-372.
- [22] Pogrebnoi, A., Kudin, L., and Kuznetsov, A.Y., *Enthalpies of formation of ions in saturated vapor over Cesium Chloride*. Russ. J. Phys. Chem. 2000. 74(10): p. 1728-1730.
- [23] Motalov, V., Pogrebnoi, A., and Kudin, L., *Molecular and ionic associates in vapor over rubidium chloride*. Russ. J. Phys. Chem. C/C of Zhurnal Fizicheskoi Khimii, 2001. 75(9): p. 1407-1412.
- [24] A. M. Pogrebnoi, L. S. Kudin, G. G. Burdukovskaya, *Mass spectrometric investigation of ion molecular equilibria in vapours over RbI, AgI and RbAg<sub>4</sub>I<sub>5</sub>*. Russ. Teplofizika vysokikh temperatur. 1992. vol. 29, pp. 907-915.
- [25] Pogrebnya, T. P., Hishamunda, J. B., Girabawe, C., & Pogrebnoi, A. M., *Theoretical study of structure, vibration spectra and thermodynamic properties of cluster ions in vapors over potassium, rubidium and cesium chlorides, in Chemistry for Sustainable Development*. 2012, Springer. p. 353-366.
- [26] Becke, A. D., *Density-functional thermochemistry. III. The role of exact exchange*. J. Chem. Phys. 1993. 98(7): p. 5648-5652.
- [27] Perdew, J. P., and Zunger, A., *Self-interaction correction to density-functional approximations for many-electron systems*. Phys. Rev. B, 1981. 23(10): p. 5048.
- [28] Perdew, J., *P hys. Rev. B 1986, 33, 8822-8824; c) JP Perdew. Phys. Rev. B, 1986. 34: p. 7406-7406.*
- [29] Perdew, J. P., *Density-functional approximation for the correlation energy of the inhomogeneous electron gas*. Physical Review B, 1986. 33(12): p. 8822.
- [30] M. W. Schmidt, K. K. Baldridge, J. A. Boatz, S. T. Elbert, M. S. Gordon, J. H. Jensen, S. Koseki, N. Matsunaga, K. A. Nguyen, S. Su, T. L. Windus, M. Dupuis, J. A. Montgomery. *General Atomic and Molecular Electronic Structure System*. J. Comput. Chem. 1993; 14:1347-1363; doi: 10.1002/jcc. 540141112.
- [31] Granovsky, A. A. Firefly version 8.1.0, [www http://classic.chem.msu.su/gran/firefly/index.html](http://classic.chem.msu.su/gran/firefly/index.html)
- [32] EMSL basis set exchange website: <https://bse.pnl.gov/bse/portal>.
- [33] Leininger, T., Nicklass, A., Kuchle, W., Stoll, H., Dolg, M., & Bergner, A., *The accuracy of the pseudopotential approximation: Non-frozen-core effects for spectroscopic constants of alkali fluorides XF (X= K, Rb, Cs)*. Chem. Phys. Lett. 1996. 255(4): p. 274-280.
- [34] Kendall, R. A., Dunning Jr, T. H., and Harrison, R. J., *Electron affinities of the first-row atoms revisited. Systematic basis sets and wave functions*. J. Chem. Phys. 1992. 96(9): p. 6796-6806.
- [35] Feller, D., *The role of databases in support of computational chemistry calculations*. J. Comp. Chem. 1996. 17(13): p. 1571-1586.

- [36] Schuchardt, K. L., Didier, B. T., Elsethagen, T., Sun, L., Gurumoorthi, V., Chase, J., and Windus, T. L., *Basis set exchange: a community database for computational sciences*. J. Chem. Info. Mod. 2007. 47(3): p. 1045-1052.
- [37] Chemcraft. Version 1.7 (build 132). G. A. Zhurko, D. A. Zhurko. HTML: [www.chemcraftprog.com](http://www.chemcraftprog.com).
- [38] Bode, B. M., and Gordon, M. S., MacMolPlt version 7.4.2. J. Mol. Graphics and Modeling, 1998; 16,133–138: <http://www.scl.ameslab.gov/MacMolPlt/>.
- [39] Tokarev, K. L. "OpenThermo", v.1.0 Beta 1 (C) ed. <http://openthermo.software.informer.com/>, 2007-2009.
- [40] Huber, K., and Herzberg, G., *Spectroscopic constants of diatomic molecules*. Van Nostrana, Princeton, NJ, 1979: p. 887-897.
- [41] Baikov, V., and Vasilevskii, K., *Infrared Spectra of Sodium, Potassium, Rubidium, and Cesium Fluoride Vapors*. Optics and Spectroscopy, 1967. 22: p. 198.
- [42] Veazey, S., and Gordy, W., *Millimeter-wave molecular-beam spectroscopy: Alkali fluorides*. Physical Review, 1965. 138(5A): p. A1303.
- [43] Hebert, A., Lovas, F., Melendres, C., Hollowell, C., Story Jr, T., & Street Jr, K., *Dipole moments of some alkali halide molecules by the molecular beam electric resonance method*. J. Chem. Phys. 1968. 48(6): p. 2824.
- [44] Hargittai, M., *Molecular structure of metal halides*. Chem. Rev. 2000. 100(6): p. 2233-2302.
- [45] Ault B. S., Andrews L., Amer, J., Chem. Soc. 1976. V. 98, p. 1591
- [46] L. V. Gurvich, V. S. Yungman, G. A. Bergman, I. V. Veitz, A. V. Gusarov, V. S. Iorish, V. Y. Leonidov, V. A. Medvedev, G. V. Belov, N. M. Aristova, L. N. Gorokhov, O. V. Dorofeeva, Y. S. Ezhov, M. E. Efimov, N. S. Krivosheya, I. I. Nazarenko, E. L. Osina, V. G. Ryabova, P. I. Tolmach, N. E. Chandamirova, E. A. Shenyavskaya, *Thermodynamic Properties of individual Substances. Ivtanthermo for Windows Database on Thermodynamic Properties of Individual Substances and Thermodynamic Modeling Software*. Version 3.0 (Glushko Thermocenter of RAS, Moscow, 1992-2000).